2015

Voigt, Reuss, Hill, and Self-Consistent Techniques for Modeling Ultrasonic Scattering

Christopher M. Kube
University of Nebraska-Lincoln, ckube@huskers.unl.edu

Joseph A. Turner
University of Nebraska-Lincoln, jaturner@unl.edu

Voigt, Reuss, Hill, and Self-Consistent Techniques for Modeling Ultrasonic Scattering

Christopher M. Kube and Joseph A. Turner

Mechanical and Materials Engineering, University of Nebraska-Lincoln, Lincoln, NE, 68588, USA

Abstract. An elastic wave propagating in a metal loses a portion of its energy from scattering caused by acoustic impedance differences existing at the boundaries of anisotropic grains. Theoretical scattering models capture this phenomena by assuming the incoming wave is described by an average elastic moduli tensor $C^0_{ijkl}(x)$ that is perturbed by a grain with elasticity $C_{ijkl}(x')$ where the scattering event occurs when $x = x'$. Previous models have assumed that $C^0_{ijkl}(x)$ is the Voigt average of the single-crystal elastic moduli tensor. However, this assumption may be incorrect because the Voigt average overestimates the wave's phase velocity. Thus, the use of alternate definitions of $C^0_{ijkl}(x)$ to describe the incoming wave is posed. Voigt, Reuss, Hill, and self-consistent definitions of $C^0_{ijkl}(x)$ are derived in the context of ultrasonic scattering models. The scattering-based models describing ultrasonic backscatter, attenuation, and diffusion are shown to be highly dependent on the definition of $C^0_{ijkl}(x)$.

Keywords: Ultrasonic scattering, grain noise, attenuation, diffusivity, Voigt, Reuss, Hill, Self-consistent, polycrystal elasticity

INTRODUCTION

Ultrasonic scattering phenomena such as backscatter, attenuation, and diffusivity have developed into practical tools for the extraction of geometric and elastic properties of the microstructure. Scattering measurements have been correlated with grain size, grain elongation, stress, and texture [1, 2, 3, 4, 5, 6]. The accuracy of the inversion depends on how well the theoretical scattering model represents the propagating wave and the microstructure. Several assumptions are found in the seminal works of the unified theory model by Stanke and Kino [7] and Weaver's model [8] describing diffusivity in polycrystals. For example, in these models and subsequent extensions, some assumptions include:

1. Microstructures can be represented by a two-point correlation function $\eta = \exp\left[-2r/\bar{d}\right]$ describing the probability that two points separated by the distance r are found within the same grain of diameter $\bar{d}$.
2. Crystallites (grains) have weak anisotropy such that scattering events can be described by a small perturbation to the mean propagating wave.
3. The statistics of the geometric and elastic properties of the microstructure can decouple and a volume average of the elastic properties represents the ensemble properties of the aggregate (ergodic hypothesis).
4. Elastic properties of the bulk material can be represented by a Voigt average of the crystallite (grain) elastic properties; elastic stiffness contributions from the grain boundaries are ignored.

Further considerations need to be made when the microstructure is more complex, i.e., elastic macro-anisotropy, multiple length scales, multiple grain phases, etc.

In this article, we attempt to improve on assumption #4, which assumes that the correct polycrystalline elasticity treatment in ultrasonic scattering models is the Voigt average. We consider the elastic formulations of Voigt, Reuss, Hill, and the self-consistent schemes defined by Hershey [9], Kröner [10], and refined by Lubarda [11] in the scope of modeling ultrasonic scattering. We will make these considerations within Weaver's model [8] by defining alternate elastic statistics governed by the elastic covariance tensor

$$\begin{aligned}\Xi^{\alpha\beta\gamma\delta}_{ijkl} &= \langle \delta C_{ijkl} \delta C_{\alpha\beta\gamma\delta} \rangle \\ &= \langle C_{ijkl} C_{\alpha\beta\gamma\delta} \rangle - \langle C_{ijkl} \rangle C^0_{\alpha\beta\gamma\delta} - \langle C_{\alpha\beta\gamma\delta} \rangle C^0_{ijkl} + C^0_{ijkl} C^0_{\alpha\beta\gamma\delta}. \end{aligned} \quad (1)$$

41st Annual Review of Progress in Quantitative Nondestructive Evaluation
AIP Conf. Proc. 1650, 926-934 (2015); doi: 10.1063/1.4914698

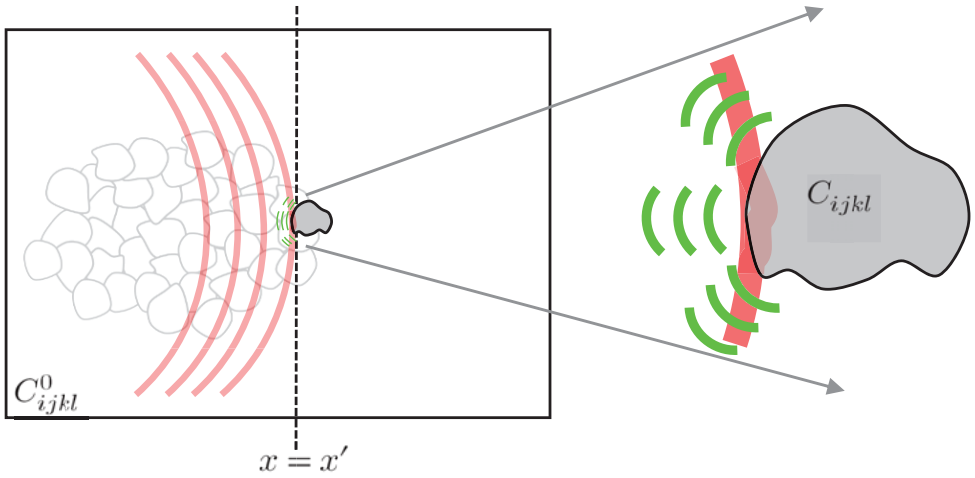

FIGURE 1. A wave is shown to have propagated through a statistically adequate number of grains such that C^0_{ijkl} defines its phase velocity. A grain with elasticity C_{ijkl} located at x' scatters a fraction of the waves energy because $C_{ijkl} \neq C^0_{ijkl}$.

In doing so, we attempt to optimize the polycrystalline elasticity contribution within Weaver's model [8]. The overall goal of this work is to improve the scattering models so that more accurate inversion measurements can be performed to find the properties of polycrystalline microstructures.

THEORETICAL DEFINITIONS OF C_{ijkl}, C^0_{ijkl}, AND $\Xi^{\alpha\beta\gamma\delta}_{ijkl}$

An elastic wave propagating in a polycrystalline medium composed of randomly oriented anisotropic grains will lose energy to scattering at the grain boundary interfaces. Scattering occurs when the wave arrives at a grain with slightly different stiffness properties. If we assume that the wave has propagated a distance x over many grains, the phase velocity of the wave can now be represented by the elastic properties of the bulk polycrystalline material C^0_{ijkl}. A grain located at x' with a local elastic modulus C_{ijkl} will scatter a portion of the wave when $x = x'$ because an acoustic impedance mismatch occurs between the interfaces described by C^0_{ijkl} and C_{ijkl}. This process is illustrated in Fig. 1, where the dashed line indicates the location of the scattering event. Traditionally, ultrasonic scattering models define C^0_{ijkl} as the Voigt average stiffness. For cubic crystallites, the Voigt average is given by

$$\begin{aligned} C^{0V}_{ijkl} &= \langle C_{ijkl} \rangle \\ &= \left(c_{12} + \frac{\nu}{5}\right)\delta_{ij}\delta_{kl} + \left(c_{44} + \frac{\nu}{5}\right)\left(\delta_{ik}\delta_{jl} + \delta_{il}\delta_{jk}\right), \end{aligned} \tag{2}$$

where $\nu = c_{11} - c_{12} - 2c_{44}$ is an anisotropy coefficient, $\langle\rangle$ indicates an average over all possible crystallite orientations, and the superscript $0V$ indicates the Voigt average. The Voigt average assumes that a uniform strain applied to the polycrystal results in an equivalent strain within a constituent crystallite, i.e., $\varepsilon_{ij} = \varepsilon^0_{ij}$. Alternatively, the Reuss average considers a uniform stress applied to the polycrystal resulting in an equivalent stress within a constituent crystallite, i.e., $\sigma_{ij} = \sigma^0_{ij}$. Thus, the Reuss average stiffness is the inverse of the average of the compliance tensor of the crystallite,

$$\begin{aligned} C^{0R}_{ijkl} &= \langle S_{ijkl} \rangle^{-1} \\ &= \left(c_{12} + \nu\frac{\nu + 2c_{44}}{3\nu + 10c_{44}}\right)\delta_{ij}\delta_{kl} + c_{44}\frac{10c_{44} + 5\nu}{10c_{44} + 3\nu}\left(\delta_{ik}\delta_{jl} + \delta_{il}\delta_{jk}\right). \end{aligned} \tag{3}$$

The Hill estimate is an arithmetic average of the Voigt and Reuss averages,

$$C^{0H}_{ijkl} = \frac{1}{2}\left(C^{0V}_{ijkl} + C^{0R}_{ijkl}\right)$$
$$= \left[c_{12} + \frac{\nu}{5}\left(1 + \frac{\nu}{3\nu + 10c_{44}}\right)\right]\delta_{ij}\delta_{kl} + \left[c_{44} + \frac{\nu}{5}\left(1 - \frac{3\nu}{2\left(3\nu + 10c_{44}\right)}\right)\right]\left(\delta_{ik}\delta_{jl} + \delta_{il}\delta_{jk}\right), \quad (4)$$

The self-consistent scheme first derived by Hershey [9] and Kröner [10] considers the grain to be an Eshelby inclusion embedded into a surrounding homogeneous medium. Lubarda considered a grain inside the polycrystal to be represented by a spherical Eshelby inclusion with cubic crystallite symmetry [11]. In this case, a uniform far-field strain on the polycrystal is linearly related to the strain inside of the grain,

$$\varepsilon_{ij} = \Lambda_{ijkl}\varepsilon^0_{kl}, \quad (5)$$

where Λ_{ijkl} is defined as a concentration tensor composed of the single-crystal elastic tensor for cubic crystals, the isotropic Eshelby tensor, and the self-consistent elastic properties of the polycrystal. It can be written as [11]

$$\Lambda_{ijkl} = \frac{1}{2}\left(\delta_{ik}\delta_{jl} + \delta_{il}\delta_{jk}\right) + h\left(\delta_{ij}\delta_{kl} + \delta_{ik}\delta_{jl} + \delta_{il}\delta_{jk} - 5a_{iu}a_{ju}a_{ku}a_{lu}\right), \quad (6)$$

where $h = \frac{1}{3\nu}\left(5c_{44} - 5C^{0SC}_{44} + \nu\right)$ and C^{0SC}_{44} is the self-consistent shear modulus of the polycrystal and is the lone positive root of the cubic equation [10], [11],

$$8\left(C^{0SC}_{44}\right)^3 + \left(9c_{12} + 10c_{44} + 5\nu\right)\left(C^{0SC}_{44}\right)^2 - c_{44}\left(3c_{12} + 14c_{44} + 7\nu\right)C^{0SC}_{44} - c_{44}\left(2c_{44} + \nu\right)\left(3c_{12} + 2c_{44} + \nu\right) = 0. \quad (7)$$

where the expected result of $C^{0SC}_{44} = c_{44}$ is obtained from Eq. (7) when the single-crystal is isotropic ($\nu = 0$). In this case, $h = 0$ and thus, $\varepsilon_{ij} = \varepsilon^0_{ij}$, and $C^{0SC}_{ijkl} = C^{iso}_{ijkl} = c_{12}\delta_{ij}\delta_{kl} + c_{44}\left(\delta_{ik}\delta_{jl} + \delta_{il}\delta_{jk}\right)$. From Eq. (5), the elastic stiffness inside of the grain defined using the self-consistent approach is

$$\hat{C}_{ijkl} = C_{ijpq}\Lambda_{pqkl}, \quad (8)$$

where $C_{ijkl} = c_{12}\delta_{ij}\delta_{kl} + c_{44}\left(\delta_{ik}\delta_{jl} + \delta_{il}\delta_{jk}\right) + \nu a_{iu}a_{ju}a_{ku}a_{lu}$ is the elastic stiffness of a cubic single-crystal. The self-consistent estimate of C^0_{ijkl} is then [11],

$$C^{0SC}_{ijkl} = \langle\hat{C}_{ijkl}\rangle,$$
$$= \left[c_{12} + \frac{\nu}{5}\left(1 + 2h\right)\right]\delta_{ij}\delta_{kl} + \left[c_{44} + \frac{\nu}{5}\left(1 - 3h\right)\right]\left(\delta_{ik}\delta_{jl} + \delta_{il}\delta_{jk}\right). \quad (9)$$

If $h = 0$, the concentration tensor $\Lambda_{ijkl} = \frac{1}{2}\left(\delta_{ik}\delta_{jl} + \delta_{il}\delta_{jk}\right)$ which results in the Voigt assumption $\varepsilon_{ij} = \varepsilon^0_{ij}$. In this case, Eq. (9) equals the Voigt definition in Eq. (2), i.e., $C^{0SC}_{ijkl} = C^{0V}_{ijkl}$. C^{0SC}_{ijkl} is defined as self-consistent because a dual formalism based on a uniform stress in the polycrystal leads to the same result. The Voigt, Reuss, Hill, and self-consistent forms for C^0_{ijkl} in Eqs. (2-4) and (9) can be used to estimate the phase velocities of long-wavelength longitudinal and shear waves,

$$\rho v^2_L = C^0_{11} \text{ and } \rho v^2_T = C^0_{44}, \quad (10)$$

respectively, where we have used reduced notation $C^0_{1111} = C^0_{11}$ and $C^0_{2323} = C^0_{44}$.

It is reasonable to assume that the correct theoretical definition of C^0_{ijkl} should accurately estimate the phase velocity of a long-wavelength wave in a polycrystalline material assuming the propagation distance contains a statistically adequate number of grains. A review of effective elastic properties of polycrystals will elucidate the homogenization schemes of Voigt, Reuss, Hill, Hashin-Shtrikman, Kröner, and many others [12, 13]. The estimates of C^0_{ijkl} for each of these schemes were compared with experimental phase velocity measurements in polycrystalline copper by Ledbetter [14]. The results compiled for longitudinal waves are given in Fig. (2) where the experimental values and error estimates are denoted by "AVG EXP VELOCITY". The Voigt and Reuss estimates are the worst, as expected, because they are the well established extremum bounds of the polycrystalline elastic properties. With this in mind we pose the following questions:

1. Should the incoming wave illustrated in Fig. (1) be defined in terms of the Voigt average C^0_{ijkl} or one of the alternatives when modeling ultrasonic scattering?
2. Should the scatterer or grain in Fig. (1) be defined by the elastic stiffness $\hat{C}_{ijkl}$ of the Eshelby inclusion?

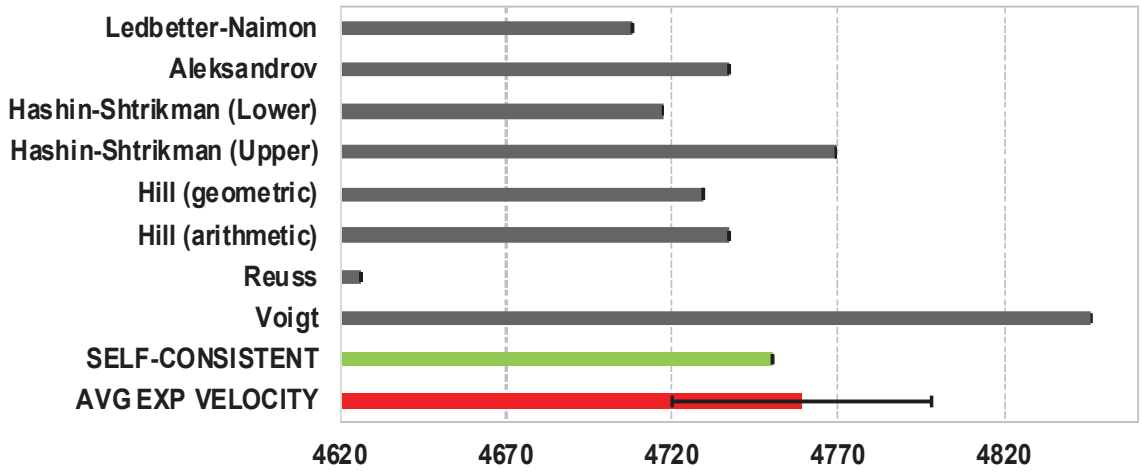

FIGURE 2. A comparison of averaging techniques used to define $C^0_{11} = \rho v_L^2$ to experimental measurements of v_L in polycrystalline copper [14]. The x-axis is the longitudinal phase velocity v_L in units of (m/s).

We substitute the different definitions of C^0_{ijkl} into the definition of the elastic covariance tensor, Eq. (1), in order to observe the influence on ultrasonic scattering models. Thus, the covariance tensor for the Voigt, Reuss, Hill, and self-consistent (SC1) models are

$$ {}^{V}\Xi^{\alpha\beta\gamma\delta}_{ijkl} = \langle C_{ijkl} C_{\alpha\beta\gamma\delta} \rangle - C^{0V}_{ijkl} C^{0V}_{\alpha\beta\gamma\delta}, \tag{11} $$

$$ {}^{R}\Xi^{\alpha\beta\gamma\delta}_{ijkl} = \langle C_{ijkl} C_{\alpha\beta\gamma\delta} \rangle - \langle C_{ijkl} \rangle C^{0R}_{\alpha\beta\gamma\delta} - \langle C_{\alpha\beta\gamma\delta} \rangle C^{0R}_{ijkl} + C^{0R}_{ijkl} C^{0R}_{\alpha\beta\gamma\delta}, \tag{12} $$

$$ {}^{H}\Xi^{\alpha\beta\gamma\delta}_{ijkl} = \langle C_{ijkl} C_{\alpha\beta\gamma\delta} \rangle - \frac{3}{4} C^{0V}_{ijkl} C^{0V}_{\alpha\beta\gamma\delta} - \frac{1}{4} C^{0V}_{ijkl} C^{0R}_{\alpha\beta\gamma\delta} - \frac{1}{4} C^{0R}_{ijkl} C^{0V}_{\alpha\beta\gamma\delta} + \frac{1}{4} C^{0R}_{ijkl} C^{0R}_{\alpha\beta\gamma\delta}, \tag{13} $$

$$ {}^{SC1}\Xi^{\alpha\beta\gamma\delta}_{ijkl} = \langle C_{ijkl} C_{\alpha\beta\gamma\delta} \rangle - \langle C_{ijkl} \rangle C^{0SC}_{\alpha\beta\gamma\delta} - \langle C_{\alpha\beta\gamma\delta} \rangle C^{0SC}_{ijkl} + C^{0SC}_{ijkl} C^{0SC}_{\alpha\beta\gamma\delta}, \tag{14} $$

respectively. The average of the squared moduli is

$$ \langle C_{ijkl} C_{\alpha\beta\gamma\delta} \rangle = \nu^2 \langle a_{iu} a_{ju} a_{ku} a_{lu} a_{\alpha v} a_{\beta v} a_{\gamma v} a_{\delta v} \rangle + \nu C^{iso}_{ijkl} \langle a_{\alpha v} a_{\beta v} a_{\gamma v} a_{\delta v} \rangle + \nu \langle a_{iu} a_{ju} a_{ku} a_{lu} \rangle C^{iso}_{\alpha\beta\gamma\delta} + C^{iso}_{ijkl} C^{iso}_{\alpha\beta\gamma\delta}. \tag{15} $$

The needed averages of the rotation matrices are

$$ \begin{aligned} \langle a_{1u} a_{1u} a_{1u} a_{1u} \rangle &= 3/5 \\ \langle a_{2u} a_{3u} a_{2u} a_{3u} \rangle &= 1/5 \\ \langle a_{1u} a_{1u} a_{1u} a_{1u} a_{1v} a_{1v} a_{1v} a_{1v} \rangle &= 41/105 \\ \langle a_{2u} a_{3u} a_{2u} a_{3u} a_{2v} a_{3v} a_{2v} a_{3v} \rangle &= 2/35. \end{aligned} \tag{16} $$

The definition of ${}^{SC1}\Xi^{\alpha\beta\gamma\delta}_{ijkl}$ considers that the incoming wave has propagated over a large number of grains that, individually, have elasticity tensors given by $\hat{C}_{ijkl}$. However, the grain at $x = x'$ is not defined by the Eshelby tensor. Thus, an alternative self-consistent scattering model (SC2) can be formulated by letting $C_{ijkl} = \hat{C}_{ijkl}$. In this case, the incoming wave in Fig. (1) is described by C^{0SC}_{ijkl} while the scatterer (grain) has a local elastic tensor $\hat{C}_{ijkl}$. Thus, the covariance of elastic moduli is

$$ \begin{aligned} {}^{SC2}\Xi^{\alpha\beta\gamma\delta}_{ijkl} &= \langle \hat{C}_{ijkl} \hat{C}_{\alpha\beta\gamma\delta} \rangle - C^{0SC}_{ijkl} C^{0SC}_{\alpha\beta\gamma\delta} \\ &= \gamma^2 \left(\langle a_{iu} a_{ju} a_{ku} a_{lu} a_{\alpha v} a_{\beta v} a_{\gamma v} a_{\delta v} \rangle - \langle a_{iu} a_{ju} a_{ku} a_{lu} \rangle \langle a_{\alpha v} a_{\beta v} a_{\gamma v} a_{\delta v} \rangle \right), \end{aligned} \tag{17} $$

where $\gamma = \nu - h(3\nu + 10c_{44})$. Note that the covariance tensors ${}^{SC1}\Xi^{\alpha\beta\gamma\delta}_{ijkl}$, and ${}^{SC2}\Xi^{\alpha\beta\gamma\delta}_{ijkl}$ are not themselves self-consistent, i.e., the covariance of elastic compliances does not lead to the covariance of elastic moduli. They are denoted self-consistent because of the use of self-consistent definitions of C^0_{ijkl}.

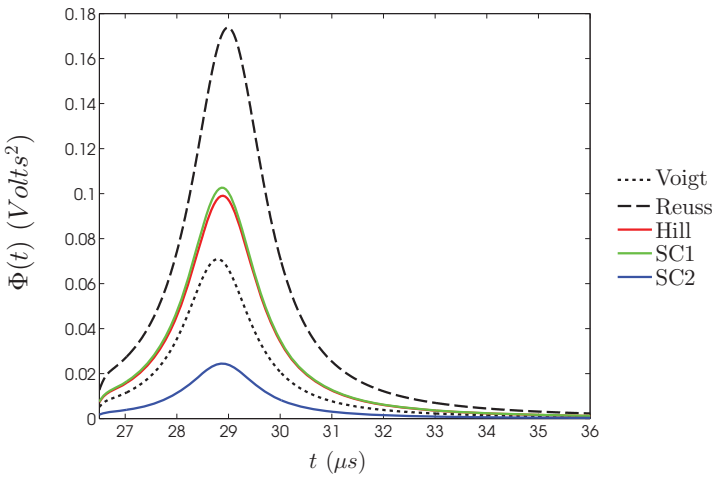

FIGURE 3. The SSR of ultrasonic backscatter for normal incidence measurements in iron using the Voigt, Reuss, Hill, self-consistent #1 and self-consistent #2 elasticity definitions.

EFFECTS ON MODELING BACKSCATTER, ATTENUATION, AND DIFFUSIVITY

The Voigt, Reuss, Hill, and two self-consistent methods are used in Eqs. (11-14) and Eq. (17), respectively, to define the covariance of elastic moduli tensor, $\Xi_{ijkl}^{\alpha\beta\gamma\delta}$, which contributes to the strength of ultrasonic grain scattering. In this section, we give examples of theoretical ultrasonic backscatter, attenuation, and diffusivity in polycrystalline iron and highlight the dependence of each averaging method. Each example assumes single-crystal elastic constants of iron as $c_{11} = 230\ GPa$, $c_{12} = 135\ GPa$, $c_{44} = 117\ GPa$ [15] and density $\rho = 7836\ kg/m^3$.

Backscatter

Ultrasonic backscatter describes the grain scattering observed on the axis of wave propagation. The scattering or grain noise is typically observed directly after a front surface reflection for pulse/echo immersion measurements. The scattered signal becomes resolvable for most iron and aluminum samples when using $5-25\ MHz$ transducers. The quantification of the scattering requires a volume average (assuming ergodicity is satisfied) that is achieved by scanning the transducer and acquiring scattered waveforms from many transducer locations. If $\phi_i(t)$ is the i^{th} collected waveform, then $\Phi(t) = \phi_{RMS}^2(t) = \left(\sum_{i=1}^{N} \phi_i^2(t)\right)/N$ gives a squared measure of the scattered energy [16]. The quantity ϕ_{RMS} was first theoretically modeled by Rose [17] and later defined by Ghoshal and Turner using Wigner transforms of the incident and scattered fields [1]. Normal incidence backscatter results in an incident wave being scattered at a scattering angle $\theta = \pi$. For this configuration, the singly-scattered response (SSR) is given by [1]

$$\Phi(t) = \Phi_0 \left[\frac{\pi}{2}\frac{\omega_0^4}{\mathrm{v}_L^8}\tilde{\eta}\left(\bar{d}, \theta=\pi\right)\Xi_{3333}^{3333}\right] \exp\left[-\frac{t^2}{\sigma^2}\right] \int_0^\infty \frac{w_0^2}{w_1(x)\, w_2(x)} \exp\left[-4\alpha_L x - \frac{4x(x-t\mathrm{v}_L)}{\sigma^2 \mathrm{v}_L^2}\right] \mathrm{d}x \qquad (18)$$

where Φ_0 is an equipment-dependent calibration parameter, $\tilde{\eta}\left(\bar{d}, \theta=\pi\right)$ is the spatial Fourier transform of the two-point correlation function, $\bar{d}$ is the mean grain diameter, α_L is the longitudinal attenuation coefficient, σ is the time duration of the input pulse, and $w_0,\ w_1(x),\ w_2(x)$ are Gaussian beam parameters. The quantity $\left[\frac{\pi}{2}\frac{\omega_0^4}{\mathrm{v}_L^8}\tilde{\eta}\left(\bar{d}, \theta=\pi\right)\Xi_{3333}^{3333}\right]$ is defined as the diffuse backscatter coefficient and contains the elastic covariance tensor Ξ_{3333}^{3333} for longitudinal-to-longitudinal backscatter. Ghoshal and Turner used a Voigt average definition for ${}^V\Xi_{3333}^{3333} = \frac{16}{525}v^2$ [1]. Figure 3 shows the SSR curves for the Voigt, Reuss, Hill, and two self-consistent definitions of Ξ_{3333}^{3333}, C_{ijkl}^0 and v_L. Each curve is generated assuming a center frequency of $\frac{\omega}{2\pi} = 9.48\ MHz$, an average grain diameter $\bar{d} = 80\ \mu m$, and single-crystal elastic constants and density of iron.

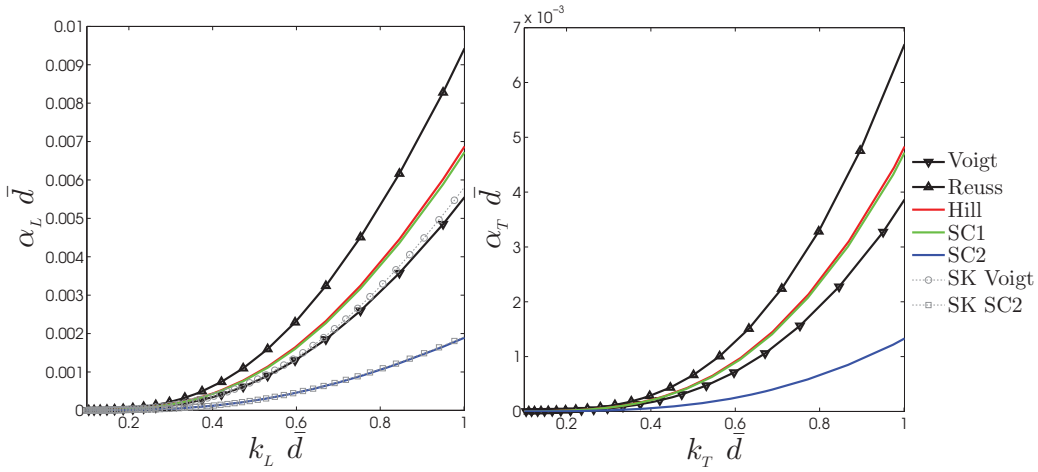

FIGURE 4. Dimensionless attenuation coefficients vs. dimensionless wave number for polycrystalline iron using the Voigt, Reuss, Hill, self-consistent #1 and self-consistent #2 elasticity definitions in Weaver's attenuation model [8]. Curves denoted with SK were generated using the model of Stanke and Kino for comparison [7].

The SSR curves defined by the Voigt and Reuss average are the lower and upper extremum, respectively, for the case where the scatterer is defined by the elasticity tensor C_{ijkl}. The Hill and SC1 SSR curves are closer to the Voigt average definition rather than the Reuss. The SC2 curve for which the grain is defined by $\hat{C}_{ijkl}$ is about a factor of three lower than the Voigt SSR. The differences in the models results in large differences when inverting the models to solve for $\bar{d}$. For example, the Voigt model would need an input grain diameter of $\bar{d} = 110\ \mu m$ to reach the same amplitude as the Hill and SC1 curves in Fig. 3.

Attenuation

The attenuation is the rate of energy loss as the wave propagates in a polycrystal and is found by integrating the scattering losses over all directions. In a statistically isotropic bulk material, the scattering can be described in terms of one angle, θ, between the incident and scattered wave directions. Additionally, an incoming longitudinal wave can mode-convert when scattered into a shear wave. Likewise, an incoming shear wave can mode-convert into a longitudinal wave. Thus, the longitudinal and shear attenuation components can be written as a sum of these combinations [8],

$$\alpha_L = \alpha_{LL} + \alpha_{LT},\ \alpha_T = \alpha_{TT} + \alpha_{TL}, \tag{19}$$

where [8]

$$\begin{aligned}
\alpha_{LL} &= \frac{\pi^2\omega^2}{2\mathrm{v}_L^8}\int_0^\pi \tilde{\eta}^{LL}(\theta)L(\theta)\sin(\theta)\,\mathrm{d}\theta,\\
\alpha_{LT} &= \frac{\pi^2\omega^2}{2\mathrm{v}_L^3\mathrm{v}_T^5}\int_0^\pi \tilde{\eta}^{LT}(\theta)[M(\theta)-L(\theta)]\sin(\theta)\,\mathrm{d}\theta,\\
\alpha_{TT} &= \frac{\pi^2\omega^2}{4\mathrm{v}_T^8}\int_0^\pi \tilde{\eta}^{TT}(\theta)[N(\theta)-2M(\theta)-L(\theta)]\sin(\theta)\,\mathrm{d}\theta,\\
\alpha_{TL} &= \frac{1}{2}\left(\frac{\mathrm{v}_T}{\mathrm{v}_L}\right)^2\alpha_{LT},
\end{aligned} \tag{20}$$

are the integrals over the scattering angle θ. The covariance of elastic moduli are contained within the inner products $L(\theta)$, $M(\theta)$, and $N(\theta)$,

$$L(\theta) = \cos^4(\theta)\,\Xi^{3333}_{3333} + 2\cos^2(\theta)\sin^2(\theta)\left(\Xi^{3333}_{1133} + 2\Xi^{3313}_{3313}\right) + \sin^4(\theta)\,\Xi^{1133}_{1133},$$

$$\begin{aligned} M(\theta) = {} & \cos^4(\theta)\left(\Xi^{3333}_{3333} + \Xi^{3323}_{3323} + \Xi^{3313}_{3313}\right) + \cos^2(\theta)\sin^2(\theta)\left(\Xi^{3333}_{1133} + \Xi^{3313}_{1113} + \Xi^{3323}_{1123} + 2\Xi^{3313}_{3313} + 2\Xi^{2313}_{2313} + 2\Xi^{1313}_{1313}\right) \\ & + \sin^4(\theta)\left(\Xi^{1133}_{1133} + \Xi^{1123}_{1123} + \Xi^{1113}_{1113}\right), \end{aligned}$$

$$\begin{aligned} N(\theta) = {} & \cos^4(\theta)\left(\Xi^{3333}_{3333} + \Xi^{3323}_{3323} + \Xi^{3313}_{3313}\right) + \cos^2(\theta)\sin^2(\theta)\left(\Xi^{1133}_{1133} + \Xi^{1123}_{1123} + \Xi^{1113}_{1113} + \Xi^{3333}_{3333} + \Xi^{3323}_{3323} + \Xi^{3313}_{3313}\right) \\ & + \sin^4(\theta)\left(\Xi^{1133}_{1133} + \Xi^{1123}_{1123} + \Xi^{1113}_{1113}\right) + \sin^2(\theta)\left(\Xi^{3312}_{3312} + \Xi^{2312}_{2312} + \Xi^{1312}_{1312}\right) + \cos^2(\theta)\left(\Xi^{3323}_{3323} + \Xi^{2323}_{2323} + \Xi^{1323}_{1323}\right) \\ & + \Xi^{3313}_{3313} + \Xi^{2313}_{2313} + \Xi^{1313}_{1313}. \end{aligned} \tag{21}$$

Using these definitions, the attenuation coefficients in Eq. (19) can be calculated using the different averaging schemes to define $\Xi^{\alpha\beta\gamma\delta}_{ijkl}$, C^0_{ijkl}, v_L, and v_T.

Figure 4 compares the longitudinal and shear attenuation coefficients for the different averaging scheme definitions using Weaver's model [8]. In addition, the Voigt and self-consistent #2 definitions for $\alpha_L\bar{d}$ were evaluated using the Stanke and Kino model (SK) [7]. Dimensionless forms were used to highlight the dependence of attenuation on both frequency ($f = \frac{\mathrm{v}k}{2\pi}$) and grain diameter ($\bar{d}$). The Hill and SC1 attenuation coefficients fall between the Voigt (lower) and Reuss (upper) curves. Similar to the backscatter results, the SC2 curve is about a factor of three lower than the Voigt curve. The similarity between the attenuation and backscatter plots is expected because normal incidence backscatter represents the on-axis loss of energy in the backward direction, which has a large component within the integrand of the attenuation definition. Traditionally, the Voigt average for obtaining theoretical attenuation coefficients has been used, but the Voigt model may give an over-estimation of the true attenuation. Preliminary evidence indicates that the self-consistent #2 formalism should be used for samples that are near ideal, i.e., high-purity samples with equiaxed and near-spherical grains [18]. Further, well-controlled, experimental measurements should be performed to confirm which model is more accurate.

Diffusivity

Ultrasonic attenuation is described by the exponential rate of spatial decay of the coherent propagating wave. The scattering out of the coherently propagating wave and subsequent multiple scattering events leads to a spatial diffusion of the energy density. The temporal decay of incoherent and multiply scattered energy is described by the diffusivity,

$$D = 6\left(\frac{1}{\mathrm{v}_L^3} + \frac{2}{\mathrm{v}_T^3}\right)^{-1} \frac{\left(\alpha_T - \alpha'_{TT} + \alpha'_{LT}\right)/\mathrm{v}_L^2 + 2\left(\alpha_L - \alpha'_{LL} + \alpha'_{TL}\right)/\mathrm{v}_T^2}{\left(\alpha_L - \alpha'_{LL}\right)\left(\alpha_T - \alpha'_{TT}\right) - \alpha'_{LT}\alpha'_{TL}}, \tag{22}$$

where the primed attenuations contain an additional factor of $\cos(\theta)$ in the integrands of Eq. (20). The expression for the diffusivity in Eq. (22) is valid for a statistically isotropic bulk material and small values of ν. It is evident that the diffusivity is related to the longitudinal and shear phase velocities and attenuations, and thus, the averaging method used to define $\Xi^{\alpha\beta\gamma\delta}_{ijkl}$ and C^0_{ijkl} (and v_L, v_T).

Figure 5 gives the theoretical estimates of the diffusivity D as a function of dimensionless frequencies for the different averaging schemes presented earlier. Again, the Hill and self-consistent #1 curves are found between the Voigt (upper) and Reuss (lower) estimates. The self-consistent #2 curve is approximately a factor of three above the Voigt curve. This result is expected because the diffusivity is inversely proportional to the attenuation [8].

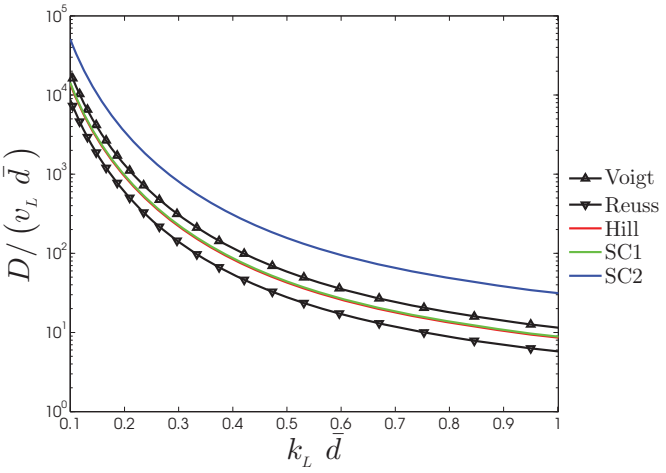

FIGURE 5. Dimensionless diffusivity coefficients vs. dimensionless wave number for polycrystalline Fe using the Voigt, Reuss, Hill, self-consistent #1 and self-consistent #2 elasticity definitions in Weaver's diffusion model [8].

CONCLUSION

In this article, the definitions of C^0_{ijkl}, which define the phase velocity in a polycrystalline medium, were formulated using the methods of Voigt, Reuss, Hill, and a self-consistent technique. Ledbetter has observed that the self-consistent definition of C^0_{ijkl} is always a better estimate than the Voigt or Reuss schemes [14]. Thus, it is appealing to attempt to model ultrasonic scattering using such techniques in order to improve their accuracy. The Voigt, Hill, Reuss, and self-consistent definitions of C^0_{ijkl} were used in the context of ultrasonic scattering models to describe the incoming wave impingent on a scattering grain. The strength of the scattering depends on the covariance of elastic moduli defined in Eq. (1), which contains C^0_{ijkl}. The Voigt and Reuss curves for each of the examples bounded the nearly identical Hill and SC1 curves. The use of Voigt definitions resulted in smaller attenuation and SSR values than the corresponding Reuss estimates. An extension of the self-consistent technique SC2 was defined by assuming that the scattering grain contained an elasticity tensor equal to an Eshelby inclusion. This formulation is physically appealing because it contains compatibility of stress and strain across the grain boundary, whereas the Voigt approach does not. Measurements of the longitudinal attenuation coefficient in a sample of high-purity copper with equiaxed grains agree well with Weaver's model using the SC2 elastic definitions [18]. The SC2 definitions within the ultrasonic backscatter, attenuation, and diffusivity models lead to large differences when compared to the Voigt model. The differences between the models could greatly influence the accuracy of inversion measurements of microstructure parameters such as grain dimensions, stress, and elastic macro-texture. Future, highly controlled, experimental measurements should attempt to confirm which of the averaging schemes is optimal.

REFERENCES

1. G. Ghoshal, J. A. Turner, and R. L. Weaver, "Wigner distribution of a transducer beam pattern within a multiple scattering formalism for heterogeneous solids," J. Acoust. Soc. Am. **122**, 2009–2021 (2007).
2. O. I. Lobkis and S. I. Rokhlin, "Characterization of polycrystals with elongated duplex microstructure by inversion of ultrasonic backscattering data," Appl. Phys. Lett. **96**, 161905 (2010).
3. C. M. Kube, H. Du, G. Ghoshal, and J. A. Turner, "Stress-dependent changes in the diffuse ultrasonic backscatter coefficient in steel: Experimental results," J. Acoust. Soc. Am. **132**, EL43–EL48 (2012).
4. P. Hu, C. M. Kube, L. W. Koester, and J. A. Turner, "Mode-converted diffuse ultrasonic backscatter," J. Acoust. Soc. Am. **134**, 982–990 (2013).
5. H. Du and J. A. Turner, "Ultrasonic attenuation in pearlitic steel," Ultrasonics, **54**, 882–887 (2014).
6. J. Li, L. Yang, and S. I. Rokhlin, "Effect of texture and grain shape on ultrasonic backscattering in polycrystals," Ultrasonics, in press (2014).

7. F. E. Stanke, and G. S. Kino, "A unified theory for elastic wave propagation in polycrystalline materials," J. Acoust. Soc. Am. **75**, 665–681 (1984).
8. R. L. Weaver, "Diffusivity of ultrasound in polycrystals," J. Mech. Phys. Solids, **38**, 55–86 (1990).
9. A. V. Hershey, "The elasticity of an isotropic aggregate of anisotropic cubic crystals," J. Appl. Mech. **21**, 236–240 (1954).
10. E. Kröner, "Berechnung der Elastischen Konstanten des Vielkristalls aus den Konstanten des Einkristalls," Z. Physik, **151**, 504–518 (1958).
11. V. A. Lubarda, "New estimates of the third-order elastic constants for isotropic aggregates of cubic crystals," J. Mech. Phys. Solids. **45**, 471–490 (1997).
12. E. Kröner, "Statistical Modeling," in *Modelling Small Deformations of Polycrystals*, edited by J. Gittus and J. Zarka (Elsevier Science Publishings CO. INC., New York, NY), pp. 229–291 (1986).
13. S. Hirsekorn, "Elastic properties of polycrystals: a review," Textures and Microstructures **12**, 1–14 (1990).
14. H. M. Ledbetter, "Sound velocities and elastic-constant averaging for polycrystalline copper," J. Phys. D: Appl. Phys. **13**, 1879–1884 (1980).
15. A. G. Every, and A. K. McCurdy, "Second and higher-order elastic constants," in *Landolt-Börnstein Numerical Data and Functional Relationships in Science and Technology New Series Group III: Crystal and Solid State Physics*, edited by O. Madelung and D. F. Nelson (Springer-Verlag, Berlin 1992), Vol. **29**.
16. F. J. Margetan, T. A. Gray, and R. B. Thompson, "A technique for quantitative measuring microstructurally induced noise," in *Review of Progress in Quantitative NDE*, edited by D. O. Thompson and D. E. Chimenti (Plenum Press, New York 1991), Vol. **10**, pp. 1721–1728.
17. J. H. Rose, "Ultrasonic backscatter from microstructure," in *Review of Progress in Quantitative NDE*, edited by D. O. Thompson and D. E. Chimenti (Plenum Press, New York 1991), Vol. **11**, pp. 1677–1684.
18. C. M. Kube, and J. A. Turner, "Scattering attenuation in polycrystals using a self-consistent approach," *Under Reveiew* (2014).